Particle fluxes in the deep Eastern Mediterranean basins: the role of ocean vertical velocities

L. Patara (1), N. Pinardi (2), C. Corselli (3), E. Malinverno (3), M. Tonani (4), L. Santoleri (5), S. Masina (1,4).

(1) Centro Euro-Mediterraneo per i Cambiamenti Climatici (CMCC), Viale Aldo Moro 44, 40138 Bologna, Italy

(2) Laboratorio SINCEM, University of Bologna, Via S. Alberto 163, 48100 Ravenna, Italy

(3) Milano-Bicocca University, Dipartimento di Scienze Geologiche e Geotecnologie, Piazza della Scienza 4, 20126 Milano, Italy

(4) Istituto Nazionale di Geofisica e Vulcanologia (INGV), Viale Aldo Moro 44, 40138 Bologna, Italy

(5) Istituto di Scienze dell'Atmosfera e del Clima – C.N.R.,Via del Fosso del Cavaliere 100, Rome, Italy

Abstract This paper analyzes the relationship between deep sedimentary fluxes and ocean current vertical velocities in an offshore area of the Ionian Sea, the deepest basin of the Eastern Mediterranean Sea. Sediment trap data are collected at 500 m and 2800 m depth in two successive moorings covering the period September 1999 – May 2001. A tight coupling is observed between the upper and deep traps and the deduced particle settling rates are larger than 200 $m\, day^{-1}$. The current vertical velocity field is computed from a high resolution Ocean General Circulation Model (OGCM) simulation and from the wind stress curl. Values are generally smaller than 1 $m\ day^{-1}$: we therefore exclude a direct effect of downward vertical velocities in determining sedimentation rates. However we find that upward vertical velocities in the subsurface layers of the water column are

significantly correlated with deep particle fluxes. We thus hypothesize that upwelling would produce an increase in upper ocean nutrient levels - thus stimulating primary productivity and grazing - a few weeks before an enhanced vertical flux is found in the sediment traps. The role of ocean vertical velocities on deep particle fluxes would therefore be indirect. High particle sedimentation rates may be attained by means of rapidly sinking fecal pellets produced by gelatinous macro-zooplankton organisms. Other sedimentation mechanisms, such as dust deposition, are also taken into account in explaining large pulses of deep particle fluxes.

1 Introduction

The Eastern Mediterranean Sea is characterized by an anti-estuarine basin scale circulation through the Sicily Channel, with the entrance of surface nutrient-depleted waters and the exiting of nutrient-enriched intermediate waters (Malanotte-Rizzoli et al. 1997; Pinardi & Masetti, 2000). Superimposed to this large scale circulation pattern, a seasonal wind-forced sub-basin scale circulation is evident (Pinardi & Navarra, 1993; Molcard et al. 2002), with the dominant north-westerly wind component giving a characteristic separation between the southern regions, dominated by anticyclonic motion, and the northern regions, dominated by cyclonic motion (Pinardi et al. 2005). The Eastern Mediterranean general circulation is moreover importantly affected by interannual scale variability mainly in response to surface fluxes (Korres et al. 2000; Demirov & Pinardi, 2002).

The open areas of the Ionian Sea, which is the deepest basin of the Eastern Mediterranean Sea, are considered to be highly oligotrophic: surface chlorophyll concentrations are generally lower than 0.5 $mg\ m^{-3}$ and a deep chlorophyll maximum is found at around 80-100 m depth (Boldrin et al. 2002; Malinverno et al. 2003; Ignatiades, 2005). The nutricline in the Eastern Mediterranean Sea is normally well below the euphotic layer. Klein et al. (1999) measure in the year 1987 a 300-400 m deep nutricline in the southeastern Ionian Sea, while Ediger & Yilmaz (1996) measure in the Levantine Basin a 600 m deep nutricline in correspondence of anticyclonic structures. In the Ionian Sea, oligotrophic features increase according to a north-south and west-east gradient (Bricaud et al. 2002; Casotti et al. 2003), in response to different water mass characteristics and possibly circulation patterns. In this oligotrophic region coccolithophores are an important constituent of the phytoplankton assemblage larger than 3 μm (Boldrin et al. 2002; Malinverno et al. 2003) and their calcitic remains give a major contribution to the calcium carbonate export to the deep layers (Ziveri et al. 2000).

Sinking mechanisms and vertical particle fluxes in open ocean areas were studied in the past by means of laboratory experiments, in situ observations and sediment traps (Honjo et al. 1984; Alldredge & Gotshalk, 1988; Asper et al. 1992; Stemmann et al. 2002; Lee et al. 2004). Aggregation inside zooplankton fecal pellets is considered to be one of the main mechanisms for organic matter sedimentation in the deep ocean (Honjo et al. 1976; Fowler et al. 1987; Knappertsbusch & Brummer, 1995). Other sinking agents include the formation of "marine snow" particles (Lampitt et al. 1993; Turner, 2002) possibly enhanced by the presence of transparent exopolymer particles (Engel, 2004). However the processes affecting particle flux magnitude and sedimentation rates in the ocean interior are not yet fully understood.

Vertical velocities of the general circulation might play a relevant role in affecting particle fluxes in two opposite ways: on one hand they could directly increase sedimentation rates through downwelling velocities; on the other hand they could produce, via upwelling velocities, an indirect effect through an enhancement of nutrient levels and primary productivity in the upper ocean.

Ekman vertical velocities, generated by the wind stress curl, were used in previous studies as a proxy of the ocean currents vertical velocities and a relation with biological patterns was found (Andersen & Prieur, 2000; Agostini & Bakun, 2002). However biogeochemical processes are directly influenced by smaller scale circulation features (Lévy et al. 2001) which might not be correctly represented by the large scale Ekman vertical velocities. These small scale features, called mesoscales, are pervasive in the Mediterranean Sea and in particular in the Ionian Sea (Robinson et al. 1987; Nittis et al. 1993).

Our goal is to understand the effect of ocean currents vertical velocities on particle fluxes observed in the ocean interior. Particles are sampled during the period 1999-2001 by means of sediment traps moored at 500 m and 2800 m depth, in two offshore sites located in the southeastern Ionian Sea, i.e. the Urania and Bannock stations. We analyze total particle flux, including all sinking particles, and coccolithophore flux in terms of the calcitic plates - the coccoliths – constituting the coccolithophores external shell.

Current vertical velocities are difficult to directly measure because of their extremely low values, which are commonly less than 1 $m\,day^{-1}$. We therefore analyze vertical velocities simulated by a high resolution Ocean General Circulation Model (OGCM) for the years 1999-2001. The OGCM vertical velocities are compared with the wind induced Ekman vertical velocities in order to verify the consistency between the two fields. The OGCM vertical velocity component is then correlated with the particle fluxes from the sediment traps.

The paper is organized as follows: Section 2 gives some details regarding the particle flux observations and the computation of the wind-induced and current vertical velocity fields. Section 3 investigates the main results of this work, concentrating on the role of ocean vertical velocities on the observed particle fluxes. In Section 4 we discuss the major findings and in Section 5 we give a few concluding remarks.

2 Methods

2.1 Particle flux data from sediment traps

Sediment trap particle flux data analyzed in this work were collected in the offshore stations Urania and Bannock located in the southeastern Ionian Sea (Figure 1). The sediment trap time series at the Urania station covers the period September 15th, 1999 - May 9th, 2001 in two successive moorings, the first one from September 15th, 1999 to June 2nd, 2000 (hereafter referred to as Mooring 1), the second one from May 30th, 2000 to May 9th, 2001 (hereafter referred to as Mooring 2). The sampling frequency varies between 10-11 days for Mooring 1 and 14-15 days for Mooring 2.

Soon after recovery, the samples were splitted on board in 8 aliquots using a pneumatic splitter. One aliquote, intended for the analysis of biogenic components, was subsequently splitted into additional sample fractions by means of a rotary splitter. Of these fractions one was filtered on a pre-weighted cellulose acetate filter, dried and then weighted. The measure of total particle flux in units of $mg\ m^{-2}\ day^{-1}$ was then calculated by knowing the sample fraction weight, the sediment trap aperture area, and the sampling frequency. Another fraction, designed for the total coccolith flux computation, was first centrifuged in order to disassemble particle aggregates, then filtered on a cellulose acetate filter and finally used for coccolith counting. The measure of total coccolith flux in units of $nC\ m^{-2}\ day^{-1}$ thus represents the sum of coccoliths sinking alone and of those deriving from disaggregated coccospheres. Additional technical details regarding the sampling procedures may be found in Malinverno et al. (in preparation).

Flux data at the Urania station are available at both 500 m and 2800 m depth for Mooring 1 and at 500 m depth for Mooring 2. At the Bannock station only total particle flux at 2800 m depth is available (see Table 1).

A few technical problems were encountered during the sediment trap deployment and recovery and during the processing of some samples. At the Urania site, a few samples from the Mooring 1 time series collected at 2800 m depth dissolved in the laboratory after being weighted and before the coccolith count. The total particle flux time series is therefore complete, whereas a few samples are missing from the coccolith flux time series. Moreover during the sediment trap recovery of Mooring 1, the last collecting bottle remained open during the ascent through the water column. The last samples of the two time series - 500 m depth and 2800 m depth - may therefore give an overestimated value of the true particle flux. At the Bannock site, the sediment trap rotation mechanism stopped after the 16th temporal interval of Mooring 1, i.e. after March 6th, 2000. Particles sinking during the remaining part of the time series (March 7th – June 2nd, 2000) were then collected in one single vial during a period of 88 days.

2.2 Vertical velocities calculation

The model used in this study is derived from the OPA code (Madec et al. 1998), it has a horizontal resolution of 1/16º×1/16º and the vertical coordinate is a full cell z-level step-wise discretization with 72 unevenly spaced levels. Vertical resolution is enhanced in the upper layers and gradually decreases with depth (Tonani et al. 2008).

The current vertical velocity field is computed as a diagnostic variable according to the continuity equation for an incompressible fluid:

$$w(z) = w(-H) - \int_{-H}^{z} \left(\frac{\partial u}{\partial x} + \frac{\partial v}{\partial y} \right) dz' \tag{1}$$

where u and v are the horizontal velocity components, w is the vertical velocity component and $-H$ is the bottom depth. The kinematic bottom boundary condition for vertical velocity can be expressed as:

$$w(-H) = -\vec{U}_h \cdot \vec{\nabla}_h H \ , \tag{2}$$

where $\vec{U}_h = (u, v)$ and $\vec{\nabla}_h = (\partial/\partial x, \partial/\partial y)$. Because of the bottom topography discretization used, $\vec{\nabla}_h H$ is equal to zero, thus vertical velocity at the ocean bottom will also be zero. The disadvantage of the z-level step-wise vertical discretization is that topographic gradients less than the grid aspect ratio are not well resolved unless very high vertical resolution is used. This may lead in some cases to small scale vertical velocities with artificially high amplitudes. This behavior was observed by Pacanowski and Gnanadesikan (1997) who compare a full cell and a partial cell discretization, which gives a better representation of topographic gradients. In the latter case the effect of (2) is mitigated and the current vertical velocity field appears to be smoother and less affected by small-scale noise.

We compare the vertical velocities computed with (1) with the Ekman vertical velocities, which are calculated as a function of the curl of the wind stress $\vec{\tau} = (\tau_x, \tau_y)$, according to:

$$w_E(x, y, \delta_E) = \frac{1}{\rho_o f} \left(\vec{k} \cdot \vec{\nabla}_h \times \vec{\tau} + \frac{\beta \tau_x}{f} \right), \tag{3}$$

where w_E is the Ekman vertical velocity, $\vec{\tau}$ is computed from ECMWF winds using a bulk formula as reported in Tonani et al. (2008), ρ_0 is the average seawater density taken as 1029 kg m^{-3}, and f is the Coriolis parameter. The β parameter, i.e. the meridional gradient of f, is computed as $\beta = 2\Omega\cos\theta/r$, where r and Ω are the Earth radius and angular velocity, and θ is the latitude.

Ekman vertical velocities are defined at the Ekman layer depth δ_E, i.e. the e-folding depth of the wind induced currents. For the Mediterranean Sea δ_E is generally between 20 and 40 m. Such an estimate is calculated using the scaling formula $\delta_E = \pi\sqrt{2A_v/|f|}$ (Pond & Pickard, 1983), where A_v is the vertical eddy coefficient for momentum, calculated in the model as a function of the Richardson number (Tonani et al. 2008), and normally variable between 10^{-2} and 10^{-3} $m^2\,sec^{-1}$.

We use the daily wind stress fields for the years 1999-2001 to compute the Ekman vertical velocity and the daily current velocity fields of the model output to compute the current vertical velocity. The comparison between the two fields is done on a monthly basis at 30 m depth.

The comparison between the current vertical velocity field and the particle flux data is done by averaging the ocean vertical velocity field on the same time intervals of the particle flux time series, i.e. 10-11 days for Mooring 1 and 14-15 days for Mooring 2.

The obtained fields are then vertically averaged between 100 m and 600 m depth: this interval allows for the surface high frequency signals to be neglected and is deep enough for the nutricline depth to be included at all seasons (Ediger & Yilmaz, 1996; Klein et al. 1999). The vertical velocity fields are then horizontally averaged on a rectangular area of 7381 km^2 and of 7471 km^2 centered on the Urania and Bannock stations respectively. We believe that these areas are large enough for model horizontal phase errors to be taken into account, while conserving the specificity of the circulation features of the two regions.

Correlations between current vertical velocities and particle fluxes are calculated both without a time lag and with a shift between time series of one and two sediment trap rotation intervals, corresponding to a lag of 11 and 22 days for Mooring 1 and to a lag of 15 and 30 days for Mooring 2. This is done in order to assess the delayed effects of ocean vertical velocities on particle fluxes. The statistical significance of the correlation coefficients is tested by applying a correlation t-test (Davis, 2002). The null hypothesis (i.e. that the correlation coefficients are statistically significant) is first of all tested at 90% confidence level: in fact, due to the smallness of the sample, there might be the risk of rejecting the null hypothesis when it should be accepted. In cases where the null hypothesis is accepted at 90% confidence level, we test the null hypothesis also at 95% and 99% confidence levels.

3 Results

3.1 Surface circulation in the Ionian Sea

In Figure 2 an average of the simulated horizontal circulation at 30 m depth for year 1999 is depicted. Modified Atlantic Water entering the Sicily Strait flows mainly eastwards towards the Levantine Sea and separates the Ionian Basin in two regions characterized by an anticyclonic circulation in the south and a prevailing weak cyclonic circulation in the north. A large meander of the Modified Atlantic Water current, called the Atlantic Ionian Stream (Robinson et al. 1999), is present in the Ionian Sea around 34.5° N with an anticyclonic curvature and a detached anticyclonic eddy to the north (up to 37° N).

The Ionian Sea was affected in the late 80s by an intensification and northward extension of the anticyclonic circulation (Malanotte-Rizzoli et al. 1999; Demirov & Pinardi, 2002). This circulation change, which is an aspect of the widespread phenomenon known as the Eastern Mediterranean Transient, appears to have recovered since the late 90s (Manca et al. 2003). The weak but cyclonic circulation north of 35° N and the large but limited in extent anticyclonic meander and northward eddy are signatures of such change, which our model succeeds to capture.

3.2 Vertical velocities in the Ionian Sea

The Ekman Vertical Velocity field (hereafter referred to as EVV) calculated according to (3), is depicted in Figure 3 for the months of November 1999 (a), June 2000 (b), November 2000 (c), and February 2001 (d), which are months overlapping with sediment trap data. EVVs have values between -0.1 and 0.1 $m\,day^{-1}$ on large portions of the Ionian Basin and exhibit a typical large scale structure consistent with the large scale wind field.

Positive values, i.e. upward EVVs, are prevalently found in the northern part of the basin, while the southern Ionian regions are typically characterized by negative values, i.e. downward EVVs. Seasonal and interannual variability is moreover evident: in February 2001 the Ionian Basin exhibits the largest areas with upward EVV, while June and November 2000 are characterized by prevailingly downward EVVs. The upward EVVs are then stronger in the northern part of the basin and in the winter season.

The Current Vertical Velocity field (hereafter referred to as CVV), calculated at 30 m depth according to (1), is depicted in Figure 4 for the months of November 1999 (a), June 2000 (b), November 2000 (c), and February 2001 (d). The CVV field is noisier with respect to the EVV field and values generally exceed 0.1 $m\ day^{-1}$ in absolute value. This is due to the intense mesoscale eddy field that modulates the Ekman vertical velocities. Consistently with the EVV field, a north-south gradient in the CVV sign and a large seasonal variability are evident, with a broadening of the areas of downward CVVs during the summer months and of the areas of upward CVVs during the winter months. The comparison between the CVV field in November 1999 and in November 2000 reveals a significant interannual variability, in agreement with the EVV field.

An overall consistency between the CVV and the EVV fields is therefore observed. However the small scale structure of the general circulation leads to a strong variability of current vertical velocities, in both space and time. The Urania and Bannock stations, despite their vicinity, may therefore be characterized by a different circulation regime because of the intense mesoscale eddy field. This variability does not appear to be correctly captured by the large scale EVV field. We thus believe that the usage of EVVs to compute correlations with sediment trap data is not suitable for our purposes.

3.3 Particle fluxes at the Urania and Bannock stations

Total Particle Flux (hereafter referred to as TPF) measured at the Urania site is depicted in Figure 5 with a light-gray line; current vertical velocity values are superimposed on the same plot with a dark-gray line. Vertical arrows located in the upper part of the panel indicate the timing of the particle flux maxima exceeding 25 $mg\ m^{-2}\ day^{-1}$.

At 500 m depth TPF is highest at the end of May - beginning of June 2000, when it attains a value of almost 160 $mg\ m^{-2}\ day^{-1}$. Secondary flux maxima of roughly 50 $mg\ m^{-2}$

day^{-1} occur in October–November 1999 and in November-December 2000 approximately. Fluxes in excess of 25 $mg\ m^{-2}\ day^{-1}$ are observed in March 2000 and April 2001. TPFs lower than 2 $mg\ m^{-2}\ day^{-1}$ occur throughout the period January-March 2001. At 2800 m depth, the highest TPF value is attained at the end of May 2000, with a value of almost 80 $mg\ m^{-2}\ day^{-1}$, whereas secondary flux maxima in excess of 20 $mg\ m^{-2}\ day^{-1}$ occur in the period included between September and November 1999.

TPF at the Urania site is on average 19 $mg\ m^{-2}\ day^{-1}$ at 500 m depth (with a standard deviation of 28 $mg\ m^{-2}\ day^{-1}$) and 15 $mg\ m^{-2}\ day^{-1}$ at 2800 m depth (with a standard deviation of 17 $mg\ m^{-2}\ day^{-1}$). The large value of the standard deviation indicates that the mean is not a robust estimate of the probability distribution due to the eventful and short time series. However this is the longest available at the moment.

Total Coccolith Flux (hereafter referred to as TCF) measured at the Urania site is depicted in Figure 6 with a light-gray line; current vertical velocity values are superimposed on the same plot with a dark-gray line. Vertical arrows located in the upper part of the panel indicate the timing of the coccolith flux maxima exceeding $5\times10^8\ nC\ m^{-2}\ day^{-1}$.

TCF at 500 m depth shows a sporadic peak attaining $3\times10^9\ nC\ m^{-2}\ day^{-1}$ at the end of May - beginning of June 2000 and secondary flux maxima in excess of $5\times10^8\ nC\ m^{-2}day^{-1}$ in October 1999 and in March 2000. At 2800 m depth TCF exhibits the largest values (in excess of $5\times10^8\ nC\ m^{-2}\ day^{-1}$) in the period September-November 1999 and at the end of May 2000. TCFs have the same order of magnitude between the upper and deep traps, i.e., $10^8\ nC\ m^{-2}\ day^{-1}$: this might be an indication of the good preservation of coccolithophore tests in the descent through the water column. TCF measured at 500 m depth during the second part of the time series is extremely low with respect to the Mooring 1 time series. We suspect that calcite dissolution might have partly occurred in the samples: therefore this part of the time series might not be fully reliable.

We may thus conclude that at the Urania site, fluxes are extremely high at the beginning of June, i.e., at the beginning of summer, and are generally large in October-November and in March-April, i.e., in the autumn and spring seasons.

TPF measured at the Bannock site is depicted in Figure 7 with a light-gray line; current vertical velocity values are superimposed on the same plot with a dark-gray line. A vertical arrow in the upper part of the panel indicates the only particle flux peak exceeding 25 $mg\ m^{-2}\ day^{-1}$.

TPF is highest at the beginning of June 2000, when it attains a value of almost 80 $mg\ m^{-2}\ day^{-1}$. There appear to be no other significant flux peaks: in the remaining part of the time series, TPF remains in fact below 4 $mg\ m^{-2}\ day^{-1}$, except for the period March 7th – June 2nd, 2000, when it is 8.84 $mg\ m^{-2}\ day^{-1}$. However, since the particles sinking throughout this period were collected in one single vial, we cannot know whether the higher TPF belongs to one single event or it is due to an overall increase of flux magnitude over the whole period. TPF at the Bannock site at 2800 m depth is on average 8 $mg\ m^{-2}\ day^{-1}$ (with a standard deviation of 16 $mg\ m^{-2}\ day^{-1}$)

TPFs measured at the Urania site are totally comparable with those observed in other off-shore sites of the Ionian Sea, while TPFs at the Bannock site are lower. Ziveri et al. (2000) observe in fact an average TPF of about 16 $mg\ m^{-2}\ day^{-1}$ at 3000 m depth at the Bannock site, while Boldrin et al. (2002) of observe an average TPF of about 17 $mg\ m^{-2}\ day^{-1}$ at 2250 m depth in the northern Ionian Sea.

Correlations between TPF and TCF are significant at 99% confidence level at both 500 m and 2800 m depth. This result may suggest an abundance of coccoliths in the total particle flux, as well as a common sinking mechanism between biogenic and lithogenic material. It is moreover evident that some of the flux “events” appear instantaneously in the upper and deep traps. Consistently, correlation coefficients calculated between the 500 m and the 2800 m depth fluxes are significant at 99% confidence level for both TPF and TCF.

Since the sediment traps at different depths are well correlated, we can compute the vertical velocity of the material sinking between 500 m and 2800 m depth. Considering the sampling resolution interval we estimate sinking velocities higher than 200 $m\ day^{-1}$ for both total particles and total coccoliths.

Correlations between the TPF of the two vertical traps are significant also with 11 days lag (99% confidence level) and with 22 days lag (95% confidence level) between the 500 m and the 2800 m depth traps. We may therefore hypothesize that a range of particle sinking velocities might be occurring in the ocean interior, with values between 70 $m\ day^{-1}$ and more than 200 $m\ day^{-1}$.

Fluxes of single coccolithophore species at the two investigated depths (Malinverno et al. in preparation) display a pattern that is consistent with this inference. In fact in the 500 m trap there is a rather distinct seasonal signal in assemblage composition, with specific abundance peaks occurring over short time intervals. In contrast in the 2800 m trap the signal is more smoothed and occurs over longer time periods.

Particle sinking speeds of more than 200 $m\ day^{-1}$ are in general agreement with other studies conducted in open areas of the Mediterranean Sea. In the northwestern Mediterranean Sea, Lee et al. (2004) observe, at 200 m depth, a dominant particle sinking regime of 200 $m\ day^{-1}$. In the northeastern Ionian Sea, Boldrin et al. (2002), estimate particle sinking speeds higher than 140 $m\ day^{-1}$ by computing the time lag between sediment trap flux peaks measured at different depths. On the contrary Ziveri et al. (2000) estimate, in the southeastern Ionian Sea, settling rates of 17-25 $m\ day^{-1}$ for coccoliths and of more than 100 $m\ day^{-1}$ for coccospheres by calculating the time lag between the 1979-1985 satellite chlorophyll maximum, and the sediment trap flux peak at 3000 m depth available for the period 1991-1994. However we may argue that satellite measurements may not be able to reach the depth of the deep chlorophyll maximum at all seasons (Morel, 1988). Moreover at the beginning of the ‘80s, there could have been different chlorophyll concentrations and phytoplankton community composition, with respect to the beginning of the ‘90s, because of the Eastern Mediterranean Transient event (Klein et al. 1999).

3.4 Correlation between current vertical velocities and particle fluxes

CVVs at the Urania site (Figure 5 and Figure 6) show positive peaks exceeding 80 $cm\ day^{-1}$ in September - October 1999 and in November 2000, whereas negative values lower than -40 $cm\ day^{-1}$ occur in June 2000 and in February 2001. Thus we observe an increase in upward motion in autumn and an increase in downward motion in summer, while winter months exhibit a different behavior between the years 2000 and 2001.

CVVs at the Bannock site (Figure 7) remain negative during most of the time series. In the period from October 1999 to May 2000, CVVs are on average -59 $cm\ day^{-1}$. Afterwards they remain negative or quite close to zero except for the period November-December 2001, when an increase of upward vertical velocities up to 50 $cm\ day^{-1}$ occurs.

Periods of upward vertical velocities are normally associated with higher particle fluxes. This behavior is observed at the Urania site in September - October 1999, in March 2000 (in the 500 m trap only) and in November 2000. Periods of downward vertical velocities appear instead to coincide with periods of low particle fluxes, as seen in February 2001 at the Urania site and throughout the period October 1999-May 2000 at the Bannock site.

An exception to this pattern occurs at the beginning of June 2000, when the high particle flux occurring at both the Urania and Bannock sites is not associated with a large increase of upward CVVs. We decided to remove the peak in June 2000 from the remaining computations: we believe in fact that mechanisms other than ocean vertical velocities are determining the strong particle fluxes observed in this period in both the Urania and Bannock sites. This hypothesis will be discussed in the next section.

In Table 2 we illustrate the correlation coefficients - and associated confidence levels - between current vertical velocities and particle fluxes. At the Urania station and during Mooring 1, correlations between coincidental time series of CVV and particle fluxes are significant at 99% confidence level for TPF at 2800 m depth and for TCF at 500 m and 2800 m depth. When the particle flux time series are lagged of one rotation interval (i.e., 11 days) with respect to the CVV time series, correlations are significant at 99% confidence level for all particle fluxes at 500 m depth, while at 2800 m depth correlations are significant at 95% confidence level. When two temporal shifts are applied (i.e. 22 days), correlations are significant at 99% confidence level for particle fluxes at 2800 m depth, while they are significant at 95% confidence level for TCF at 500 m and not significant for TPF at 500 m depth. During Mooring 2, TPF is correlated with ocean vertical velocities at 95% confidence level for coincidental time series and at 90% confidence level for lagged time series. TCF does not exhibit instead significant correlations (not shown): this behavior might be due to partial calcite dissolution in the samples.

At the Bannock station and during Mooring 1, a correlation significant at 90% confidence level exists on coincidental time series, while on time series shifted of two rotation intervals the significance increases to 99% confidence level. During Mooring 2, correlations between CVV and TPF are not significant.

We thus conclude that an overall significant positive correlation exists at both the Urania and Bannock stations between particle fluxes and current vertical velocities. Furthermore during Mooring 1 we observe that at 500 m depth correlations are higher with 11 days lag than with 22 days lag, while at 2800 m depth correlations are higher with 22 days lag than with 11 days lag. This behavior might suggest a delay process between CVV and particle fluxes, as will be discussed in the next section.

4 Discussion

4.1 Upwelling-enhanced deep particle fluxes

The positive correlation between upward vertical velocities and particle fluxes might seem at first sight surprising. We might think that downward vertical velocities should enhance particle fluxes through an increase of vertical sinking velocities. To explain this apparent inconsistency, we must first of all consider that the particle sinking rates estimated from the sediment traps are two orders of magnitude higher than the ocean vertical velocities calculated from the model output. We thus have to exclude a direct effect of ocean vertical velocities on deep particle fluxes and we speculate that, in the region analyzed in this study, another sedimentation mechanism is at work.

The high sinking rates estimated in this work might be obtained by means of biological aggregation of particles inside fecal pellets produced by macro-zooplankton. Mazzocchi et al. (2003) detect in spring 1999 an increase in abundance of suspension filter feeders (mainly appendicularians, salps, and doliolids) in the eastern Ionian Sea. Pelagic tunicates feed on unicellular phytoplankton by filtering large volumes of water and are adapted to dilute environments where they exhibit a rapid population growth if environmental conditions are favorable (Alldredge & Madin, 1982). Pelagic tunicates produce fecal pellets which sink very rapidly, with a range between 242 and 2700 $m\ day^{-1}$ for salps (Bruland & Silver, 1981; Yoon et al. 1996; Yoon et al. 2001) and between 25 and 504 $m\ day^{-1}$ for appendicularians and doliolids (Turner, 2002 and references therein).

We hypothesize that the following sedimentation mechanism might be occurring in the open areas of the Eastern Mediterranean Sea. If upward vertical velocities are capable of producing a nutricline uplift in the euphotic layer, coccolithophores will take advantage of the nutrient increase giving rise to an enhancement of primary production, which would eventually stimulate grazing. The calcitic constituents of coccolithophores would then sink through the water column inside rapidly sinking fecal pellets or other large particles and would be collected by sediment traps (see Figure 8). Considering the sampling resolution of the sediment traps (10-11 days for Mooring 1) we realize that the described mechanism of upwelling-enhanced deep particle fluxes is very fast.

Not only TCFs, but also TPFs are correlated with ocean vertical velocities on coincidental time series. This observation is corroborating the hypothesis of a common sinking mechanism among the various components of the total particle flux, e.g. through biological aggregation inside macro-zooplankton fecal pellets.

Considering the significant correlations between ocean vertical velocities and lagged particle flux time series we suggest that a spectrum of particle sinking rates exists in the ocean interior. This conclusion was also inferred from the correlation values obtained between lagged particle flux time series at 500 m and at 2800 m depth. Associated with the fast sinking regime of more than 200 $m\ day^{-1}$, there appears to be a slower regime of about 100 $m\ day^{-1}$, which might be responsible for the significant correlations between ocean vertical velocities and particle fluxes with 11 days lag at 500 m depth and with 22 days lag at 2800 m depth.

The lack of significant correlations at the Bannock site during Mooring 2 suggests that the described model of upwelling-enhanced deep particle fluxes is not always fully applicable. It is possible that other physical and biological processes are influencing the observed particle fluxes. These mechanisms might include horizontal advection and vertical mixing in the upper ocean. Seasonal variability of macro-zooplankton abundance might also lead to varying sinking regimes throughout the year. Finally we cannot exclude that technical issues related to trapping efficiency of the sediment traps might have affected the particle flux time series.

4.2 Dust-enhanced deep particle fluxes

At the end of May-beginning of June, 2000 a strong particle flux peak occurs at both the Urania and Bannock sites (Figure 5, 6 and 7). This particle flux peak is not associated with an increase of upward CVVs. We suggest that this particle flux peak is due to a strong dust event, which would enhance lithogenic and possibly biogenic flux.

Saharan dust transport over the Mediterranean occurs frequently in spring and summer in the form of non-continuous “pulses” (Kubilay et al. 2000). The effect of the Saharan dust particles on biogenic flux may be double: firstly it may represent an important source of nutrients in the euphotic layer (Markaki et al. 2003; Herut et al. 2005). Secondly lithogenic particles may have a ballasting effect which would promote the sinking of the biogenic particles within the ocean interior (Klaas & Archer, 2002).

A time series of SeaWiFS TrueColor satellite images for the period May 22nd - July 13th, 2000 is available (Figure 9). Images reveal an intense dust event, associated with an atmospheric cyclonic structure, occurring in the period May 22nd - 27th, 2000 in the southeastern Ionian Sea. The Urania and Bannock sites are on the direct trajectory of this dust phenomenon. We can therefore reasonably consider this event as responsible for the high flux peak detected in the sediment trap starting at the end of May 2000.

5 Conclusions

The mechanisms of sedimentary particle fluxes in the deep Urania and Bannock sites were studied by means of sediment trap records and model simulated vertical velocities.

The current vertical velocities for the area of the Ionian Sea have a large mesoscale signal that is superimposed to a seasonally varying Ekman vertical velocity field at low amplitude. It is found that current vertical velocities at the Urania site are positive (upward motion) in autumn and in spring when pulses of total particle fluxes are found in the water column at 500 m and 2800 m depth.

From sediment trap data the sinking velocities of TPF and TCF are estimated to be 100-200 *m* day^{-1} while current vertical velocities are estimated to be around 1 *m* day^{-1}. This observation brought us to envisage a tight coupling between surface layers and deep ocean through particle aggregation mechanisms. We found evidence that fast sinking rates of organic material in the deep ocean are connected to both lithogenic and biological aggregation mechanism that transfer particles rapidly in the deep water column.

In synthesis two emerging fast sinking mechanisms have been captured:

1. Pulses of primary production, triggered by upward current vertical velocities, followed by grazing and macro-zooplankton-related biogenic flux that rapidly conveys the material in the deep ocean.
2. Large Saharan dust events that fertilize the upper ocean and possibly contribute to aggregation of organic material, thus producing large sedimentation fluxes.

If these mechanisms are at work in other open-ocean areas, it is possible to argue that the carbon export to the deep ocean is larger in the cyclonic gyres of the ocean general circulation and during the months of maximum upward vertical velocities. The fast sinking rates estimated in this study are moreover an evidence of the efficiency of the biological pump in sequestering organic carbon from the surface layers of the open areas of the Mediterranean Sea. Further work is however to be done to unravel the relevant physical features of the marine environment capable of affecting the deep particle fluxes.

Acknowledgements

Sediment trap samples were available for the study of biogenic particles within an Italian-Dutch cooperation agreement. Mooring equipment was made available by NWO/ALW, through the Dutch Marine Research Facilities at NIOZ; ship-time was funded alternatively by NWO and the Italian CoNISMa (National Interuniversity Consortium for Marine Sciences). The study of biogenic particles was performed within the European Project BIODEEP (BIOtechnologies from the DEEP, EVK3-2000-00042).

References

Agostini, V. N. and Bakun, A.: ‘Ocean triads’ in the Mediterranean Sea: physical mechanisms potentially structuring reproductive habitat suitability (with example application to European anchovy, *Engraulis encrasicolus*), Fish Oceanography, 11(3), 129-142, 2002.

Alldredge, A.L. and Gotschalk, C.: In situ settling behavior of marine snow, Limnology and Oceanography, 33(3), 339-351, 1988.

Alldredge, A.L. and Madin, L.P.: Pelagic tunicates – unique herbivors in marine plankton, Biosciences, 32, 655-663, 1982.

Andersen, V. and Prieur, L.: One-month study in the open NW Mediterranean Sea (DYNAPROC experiment, May 1995): overview of the hydrobiogeochemical structures and effects of wind events, Deep Sea Research Part I, 47 (3), 397-422, 2000.

Asper, V.L., Deuser, W.G., Knauer, G.A., Lohrenz, S.E.: Rapid coupling of sinking particle fluxes between surface and deep ocean waters, Nature, 357, 670-672, 1992.

Boldrin, A., Miserocchi, S., Rabitti, S., Turchetto, M.M. Balboni, V., Socal, G.: Particulate matter in the southern Adriatic and Ionian Sea: characterization and downward fluxes, Journal of Marine Systems, 33-34, 389-410, 2002.

Bricaud, A., Bosc, E., Antoine, D.: Algal biomass and sea surface temperature in the Mediterranean Basin. Intercomparison of data from various satellite sensors, and implications for primary production estimates, Remote Sensing of Environment, 81(2-3), 163-178, 2002.

Bruland, K.W. and Silver, M.W.: Sinking rates of fecal pellets from gelatinous zooplankton (salps, pteropods and doliolids), Marine Biology, 63, 295-300, 1981.

Casotti, R., Landolfi, A., Brunet, C., D'Ortenzio, F., Mangoni, O, Ribera d'Alcalà, M., Denis, M.: Composition and dynamics of the phytoplankton of the Ionian Sea (eastern Mediterranean), Journal of Geophysical Research–Oceans, 108(9), pp. PBE 17-1, 2003.

Davis, J.C.: Statistics and Data Analysis in Geology, Wiley & Sons, 3rd edition, pp. 74-75, pp. 602-603, 2002.

Demirov, E. and Pinardi, N.: Simulation of the Mediterranean Sea circulation from 1979 to 1993: Part I. The interannual variability, Journal of Marine Systems, 33-34, 23-50, 2002.

Ediger, D., Yilmaz, A.: Characteristics of deep chlorophyll maximum in the Northeastern Mediterranean with respect to environmental conditions, Journal of Marine Systems, 9 (3-4), 291-303, 1996.

Engel, A.: Distribution of transparent exopolymer particles (TEP) in the northeast Atlantic Ocean and their potential significance for aggregation processes, Deep-Sea Research Part I, 51(1), 83-92, 2004.

Fowler, S.W., Buat-Menard, P., Yokoyama, Y., Ballestra, S., Holm, E., Van Nguyen, H.: Rapid removal of Chernobyl fallout from Mediterranean surface waters by biological activity, Nature 329(3), 56-58, 1987.

Herut, B., Zohary, T., Krom, M. D., Mantoura, R.F.C., Pitta, P., Psarra, S., Rassoulzadegan, F., Tanaka, T., Thingstad, T. F.: Response of East Mediterranean surface water to Saharan dust: On-board microcosm experiment and field observations, Deep-Sea Research Part II – Topical Studies in Oceanography, 52(22-23), 3024-3040, 2005.

Honjo, S., Coccoliths: Production, Transportation and Sedimentation, Marine Micropaleontology, 1, 65-79, 1976.

Honjo, S., Doherty, K. W., Agrawal, Y. C., Asper, V. L.: Direct optical assessment of large amorphous aggregates (marine snow) in the deep ocean, Deep-Sea Research, 37, 67-76, 1984.

Ignatiades, L.: Scaling the trophic status of the Aegean Sea, eastern Mediterranean, Journal of Sea Research, 54, 51-57, 2005.

Klaas, C. and Archer, D. E.: Association of sinking organic matter with various types of mineral ballast in the deep sea: implications for the rain ratio, Global Biogeochemical Cycles, 16, Dec 5, 2002

Klein, B., Roether, W., Manca, B. B., Bregant, D., Beitzel, V., Kovacevic, V., Lucchetta, A.: The large deep water transient in the Eastern Mediterranean, Deep-Sea Research Part I, 46, 371-414, 1999.

Knappertsbusch, M. and Brummer, G.-J.A.: A sediment trap investigation of sinking coccolithophorids in the North Atlantic, Deep-Sea Research Part I, 42, 1083-1109, 1995.

Korres, G., Pinardi, N., Lascaratos, A.: The Ocean Response to Low-Frequency Interannual Atmospheric Variability in the Mediterranean Sea. Part I: Sensitivity Experiments and Energy Analysis, Journal of Climate, 13(4), 705-731, 2000.

Kubilay, N., Nickovic, S., Moulin, C., Dulac, F.: An illustration of the transport and deposition of mineral dust onto the Eastern Mediterranean, Atmospheric Environment, 34, 1293-1303, 2000.

Lampitt, R. S., Hillier, W. R., Challenor, P. G.: Seasonal and diel variation in the open ocean concentration of marine snow aggregates, Nature, 362, 737-739, 1993.

Lee, C., Armstrong, R. A., Beck, A., Cochran, J. K., Wakeham, S. G., Peterson, M. L., Miquel, J.-C.: MEDFLUX: Association of organic matter with ballast minerals in sinking particles. American Geophysical Union, Fall Meeting 2004, abstract # OS52A – 02, 2004.

Lévy, M., Mémery, L., Madec, G., The onset of a bloom after deep winter convection in the northwestern Mediterranean sea: mesoscale process study with a primitive equation model, Journal of Marine Systems, 16 (1-2), 7-21, 1998.

Madec, G., Delecluse, P., Imbard, M., Lévy, C.: OPA8.1 Ocean General Circulation Model reference manual. Note du Pole de modélization, Institut Pierre-Simon Laplace (IPSL), France, 11, 1998.

Malanotte-Rizzoli, P., Manca, B.B., Ribera d'Alcalà, M., Theocharis, A., Bergamasco, A., Bregant, D., Budillon, G., Civitarese, G., Georgopoulos, D., Michelato, A., Sansone, E., Scarazzato, P., Souvermezoglou, E.: A synthesis of the Ionian Sea hydrography, circulation and water mass pathways during POEM-Phase I, Progress in Oceanography 39, 153-107, 1997.

Malanotte-Rizzoli, P., Manca, B.B., Ribera d'Alcala, M., Theocharis, A., Brenner, S., Budillon, G., Oszoy, E.: The Eastern Mediterranean in the 80s and in the 90s: the big transition in the intermediate and deep circulations, Dynamics of Atmosphere and Oceans 29, 365-395, 1999.

Malinverno, E., Ziveri, P., Corselli, C.: Coccolithophorid distribution in the Ionian Sea and its relationship to eastern Mediterranean circulation during late fall to early winter 1997, Journal of Geophysical Research - Oceans, 108, Sep 12, 2003.

Manca, B.B., Budillon, G., Scarazzato, P., Ursella, L.: Evolution of dynamics in the Eastern Mediterranean affecting water mass structures and properties in the Ionian and Adriatic Seas. Journal of Geophysical Research, 108, 8102, 2003.

Markaki, Z., Oikonomou, K., Kocak, M., Kouvarakis, G., Chaniotaki, A., Kubilay, N., Mihalopoulos, N.: Atmospheric deposition of inorganic phosphorus in the Levantine Basin, eastern Mediterranean: Spatial and temporal variability and its role in seawater productivity, Limnology and Oceanography, 48 (4), 1557-1568, 2003.

Mazzocchi, M.G.; Nervegna, D.; D'Elia, G.; Di Capua, I.; Aguzzi, L.; Boldrin, A., 2003. Spring mesozooplankton communities in the epipelagic Ionian Sea in relation to the Eastern Mediterranean Transient, Journal of Geophysical Research – Oceans, 108, Sep 24, 2003.

Molcard, A., Pinardi, N., Iskandarani, M., Haidvogel, D.B.: Wind driven general circulation of the Mediterranean Sea simulated with a Spectral Element Ocean Model, Dynamics of Atmospheres and Oceans, 35, 97-130, 2002.

Morel, A.: Optical modeling of the Upper Ocean in Relation to Its Biogenous Matter Content (Case I Waters), Journal of Geophysical Research, 93 (C9), 10749-10768, 1988.

Nittis, K., Pinardi, N., Lascaratos, A.: Characteristics of the summer 1987 flow-field in the Ionian Sea, Journal of Geophysical Research-Oceans, 98 (C6), 10171-10184, 1993.

Pacanowski, R.C. and Gnanadesikan, A.: Transient response in a z-level ocean model that resolves topography with partial cells, Monthly Weather Review, 126 (12), 3248-3270, 1998.

Pinardi, N. and Navarra, A.: Baroclinic wind adjustment processes in the Mediterranean Sea, Deep-Sea Research Part II, 40 (6), 1299-1326, 1993.

Pinardi, N. and Masetti, E.:Variability of the large scale general circulation of the Mediterranean Sea from observations and modelling: a review, Palaeogeography, Palaeoclimatology, Palaeoecology, 158, 153-174, 2000.

Pinardi, N., Arneri, E., Crise, A., Ravaioli, M., Zavatarelli, M.: The physical, sedimentary and ecological structure and variability of shelf areas in the Mediterranean Sea, in: The Sea, Vol. 14, Harvard University Press, 2005.

Pond, S., Pickard, G.L.: Introductory Dynamical Oceanography, 2nd edition, Ed.Elsevier Butterworth-Heinemann, 1983.

Robinson, A.R., Hecht, A., Pinardi, N., Bishop, J., Leslie, W.G., Rosentroub, Z., Mariano, A.J., Brenner, S.: Small synoptic mesoscale eddies and energetic variability of the Eastern Levantine Basin. Nature, 327 (6118), 131-134, 1987.

Robinson, A.R., Sellschopp, J., Warn-Varnas, A., Leslie, W.G., Lozano, C.J., Haley, P.J., Anderson, L.A., Lermusiaux, P.F.J.: The Atlantic Ionian Stream, Journal of Marine Systems, 20 (1-4), 129-156 (28), 1999.

Stemmann, L., Gorsky, G., Marty, J. C., Picheral, M., Miquel, J.-C.: Four-year study of large-particle vertical distribution (0-1000 m) in the NW Mediterranean Sea in relation to hydrology, phytoplankton, and vertical flux, Deep-Sea Research Part II, 49, 2143-2162, 2002.

Tonani, M., Pinardi. N., Dobricic, S., Pujol. I., Fratianni, C.: A high-resolution free-surface model of the Mediterranean Sea, Ocean Sciences, 4, 1-14, 2008.

Turner, J. T., Zooplankton fecal pellets, marine snow and sinking phytoplankton blooms, Aquatic Microbial Ecology, 27, 57-102, 2002.

Yoon, W. D., Marty, J. C., Sylvain, D., Nival, P.: Degradation of faecal pellets in Pegea confoederata (Salpidae, Thaliacea) and its implication in the vertical flux of organic matter, Journal of Experimental Marine Biology and Ecology, 203, 147-177, 1996.

Yoon, W. D., Kim, S. K., Han, K. N.: Morphology and sinking velocities of fecal pellets of copepod, molluscan, euphasiid, and salp taxa in the northeastern tropical Atlantic, Marine Biology, 139, 923-928, 2001.

Ziveri, P., Rutten, A., de Lange, G. J., Thomson, J., Corselli, C.: Present-day coccolith fluxes recorded in central eastern Mediterranean sediment traps and surface sediments, Palaeogeography, Palaeoclimatology, Palaeoecology, 158, 175-195, 2000.

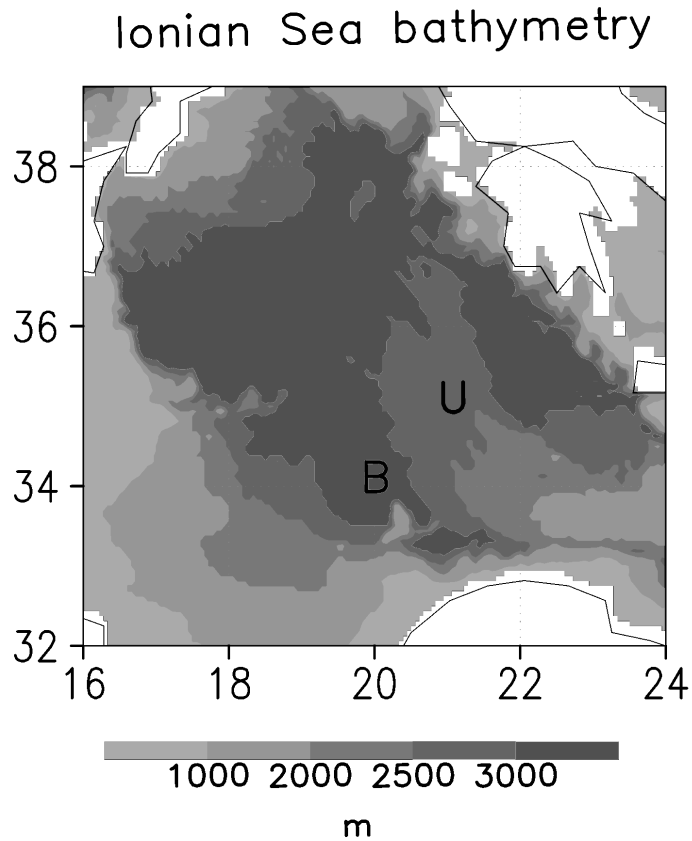

Figure 1 Ionian Sea bathymetry and sediment trap sites locations. U = Urania Basin (lat 35.2º N, lon 21.2º E), B = Bannock Basin (lat 34.2º N, lon 20º E).

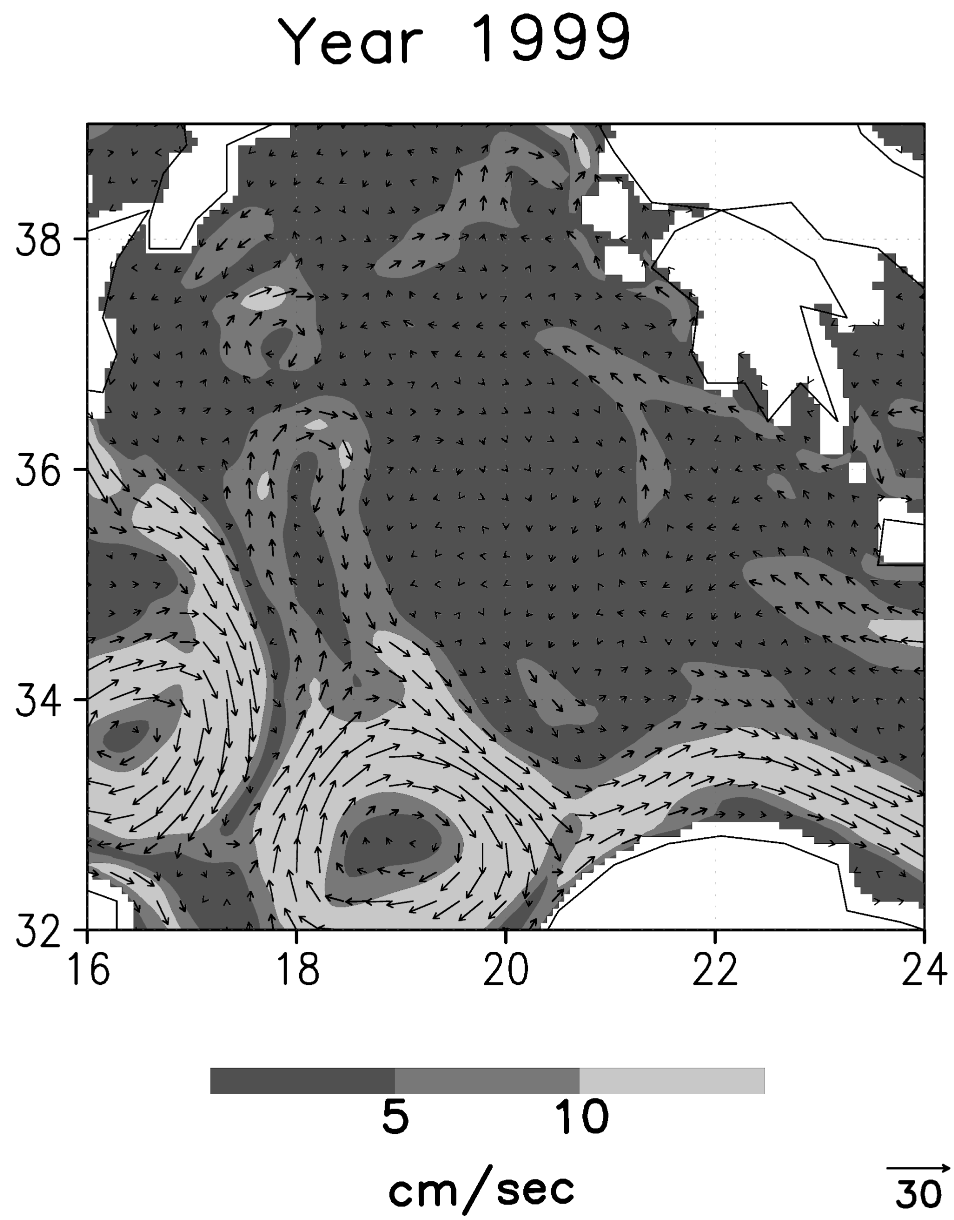

Figure 2 Year 1999 annual average of the horizontal currents [cm sec^{-1}] at 30 m depth. The arrow length indicates the 30 cm sec^{-1} velocity.

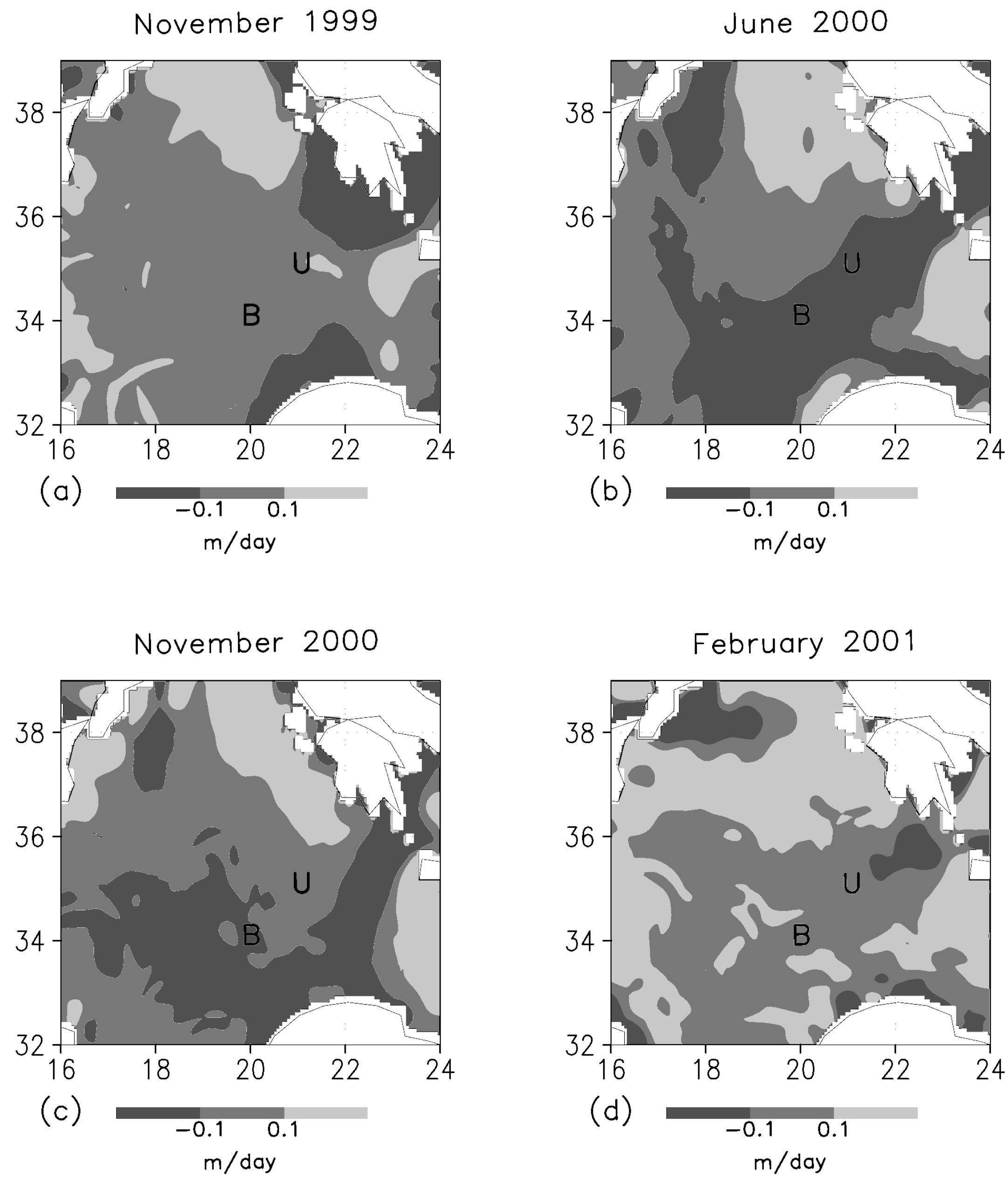

Figure 3 Ekman vertical velocities [m day^{-1}]: (a) November 1999 (b) June 2000 (c) November 2000 and (d) February 2001. In letters we indicate the position of the Urania (U) and Bannock (B) stations.

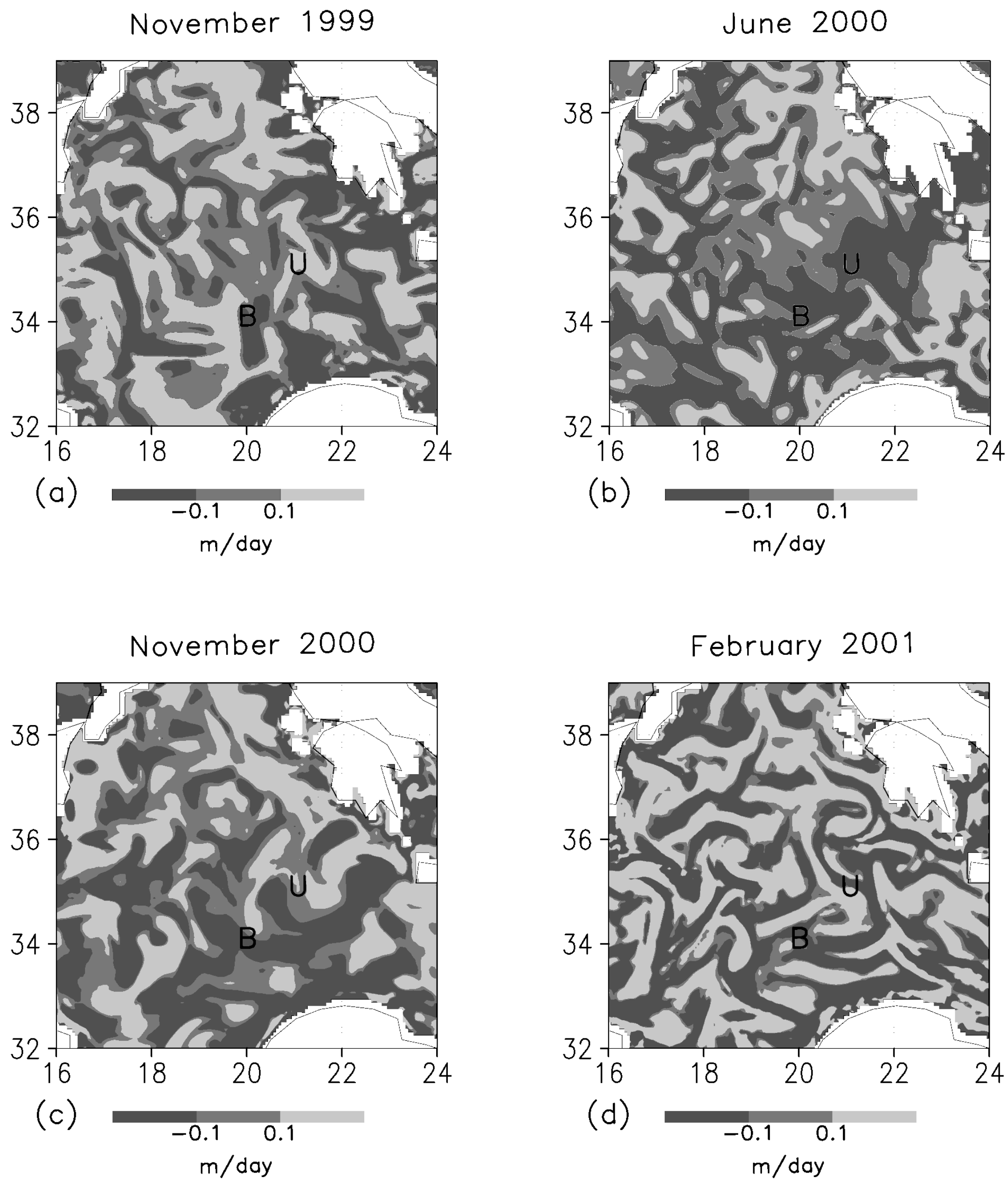

Figure 4 Ocean currents vertical velocities [m day^{-1}]: (a) November 1999 (b) June 2000 (c) November 2000 and (d) February 2001. In letters we indicate the position of the Urania (U) and Bannock (B) stations.

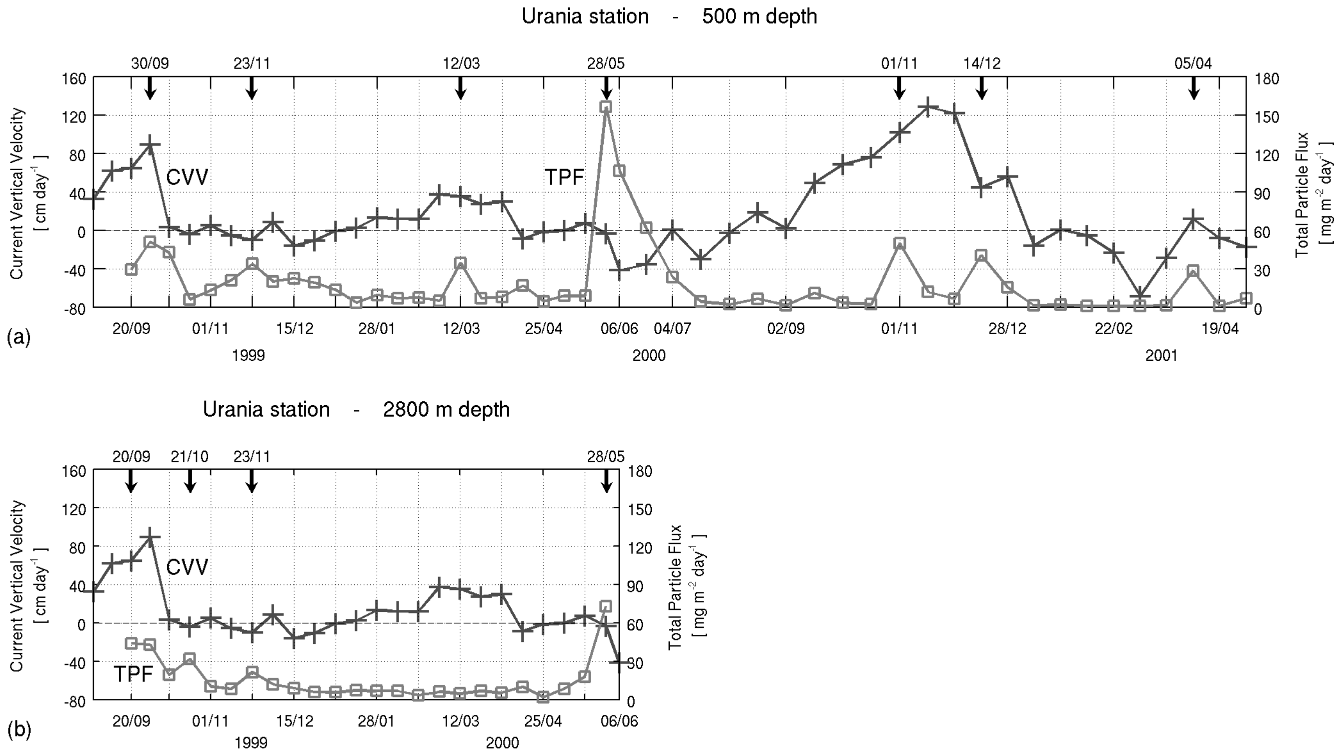

Figure 5 Total Particle Flux (TPF) and Current Vertical Velocity (CVV) at the Urania site for Mooring 1 (September 15th, 1999 to June 2nd, 2000) and for Mooring 2 (May 30th, 2000 to May 9th, 2001). Light-gray line: Total Particle Flux [mg m^{-2} day^{-1}] at 500 m depth (top) and at 2800 m depth (bottom). Dark-gray line: Current Vertical Velocity [cm day^{-1}] integrated on the 100-600 m depth interval. With black arrows we indicate Total Particle Fluxes exceeding 25 mg m^{-2} day^{-1}.

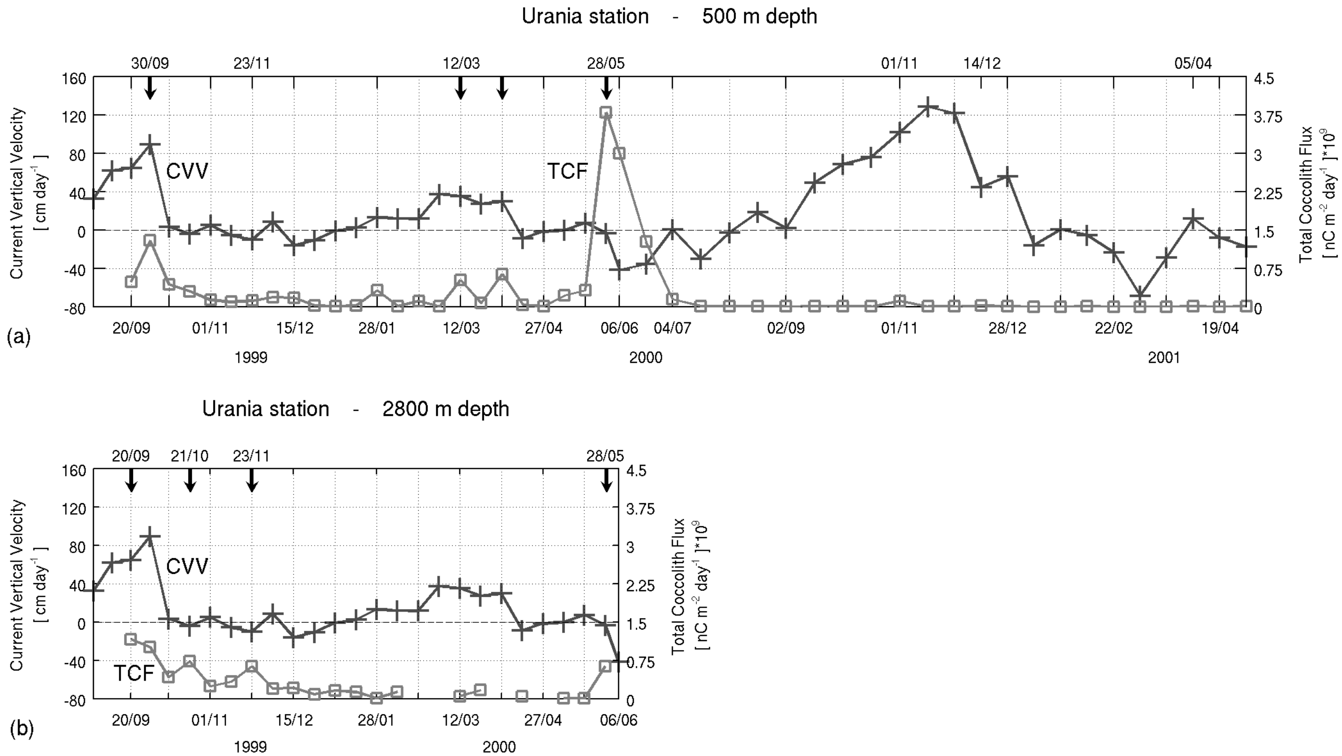

Figure 6 Total Cocolith Flux (TCF) and Current Vertical Velocity (CVV) at the Urania site for Mooring 1 (September 15^{th}, 1999 to June 2^{nd}, 2000) and Mooring 2 (May 30^{th}, 2000 to May 9^{th}, 2001). Light-gray line: Total Coccolith Flux [nC m^{-2} day^{-1}]$\times 10^9$ at 500 m depth (top) and at 2800 m depth (bottom). Dark-gray line: Current Vertical Velocity [cm day^{-1}] integrated on the 100-600 m depth interval. With black arrows we indicate Total Coccolith Fluxes exceeding 5×10^8 nC m^{-2} day^{-1}.

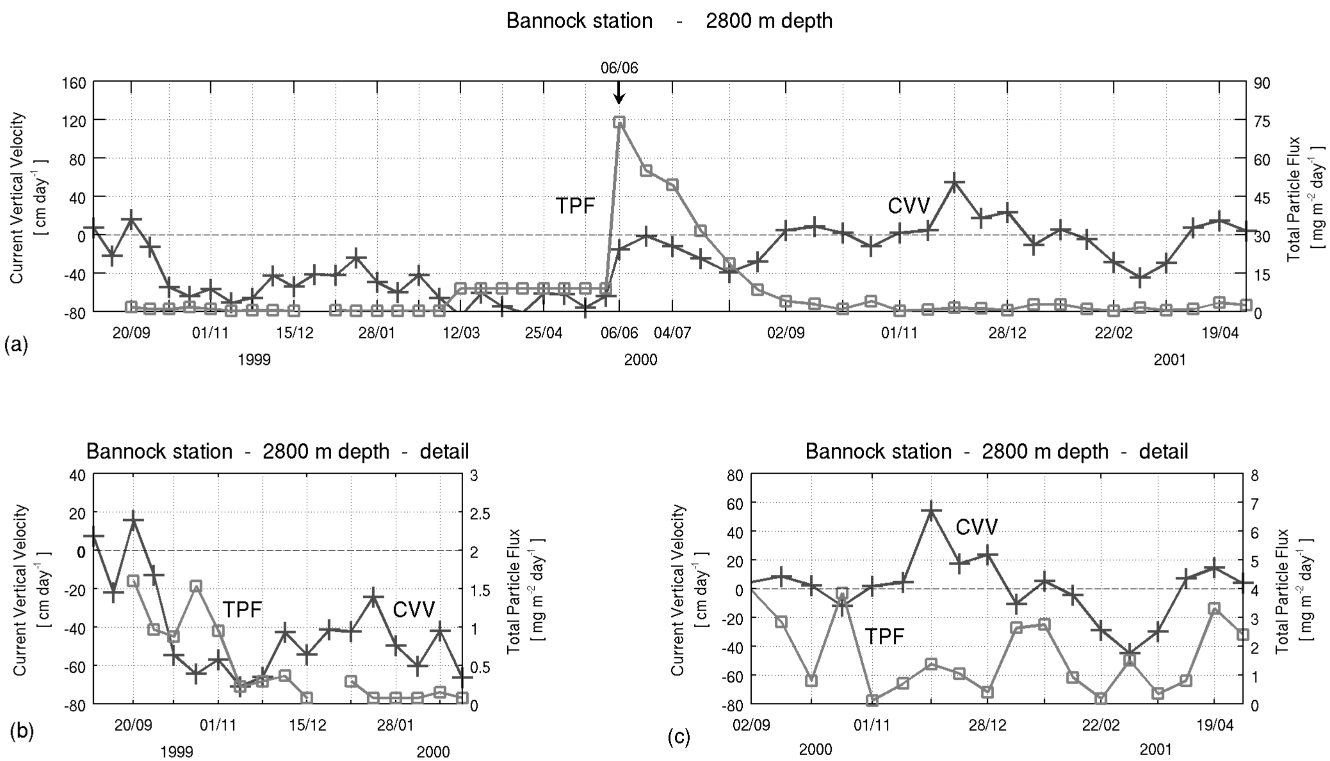

Figure 7 Total Particle Flux (TPF) and Current Vertical Velocity (CVV) at the Bannock site for Mooring 1 (September 15th, 1999 to June 2nd, 2000) and Mooring 2 (May 30th, 2000 to May 9th, 2001). Light-gray line: Total Particle Flux [mg m^{-2} day^{-1}] at 2800 m depth. Dark-gray line: Current Vertical Velocities [cm day^{-1}] integrated on the 100-600 m depth interval Top: whole time series. Bottom: decreased y-axis scale in the periods of low particle fluxes. With black arrows we indicate Total Particle Fluxes exceeding 25 mg m^{-2} day^{-1}.

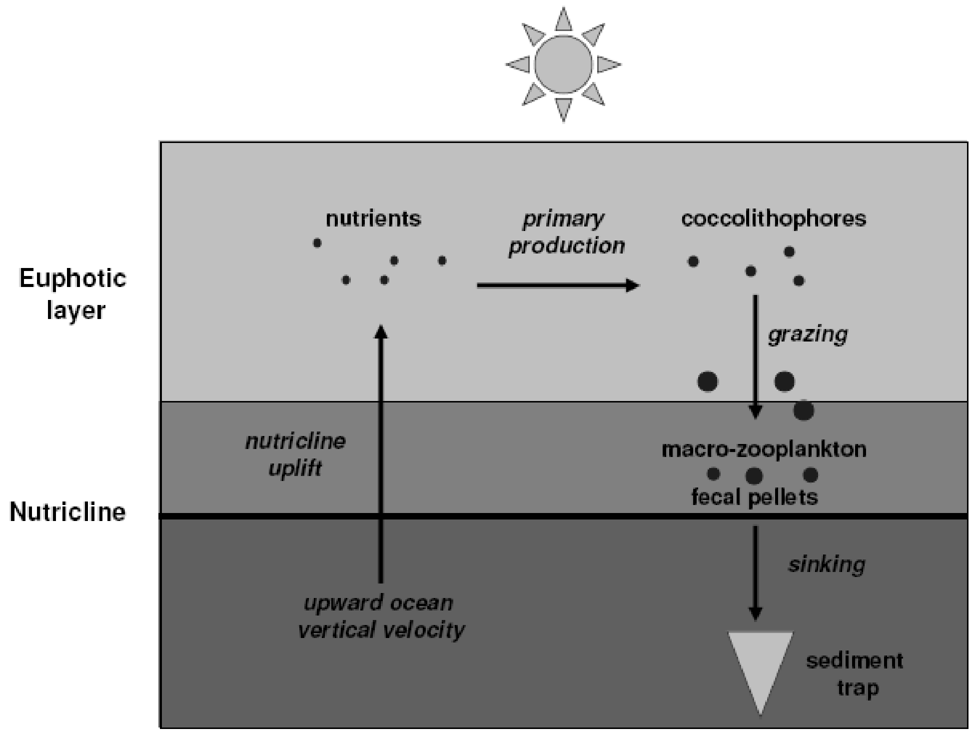

Figure 8 Model of upwelling-enhanced deep particle fluxes. A nutricline uplift by means of upward vertical velocities leads to a nutrient increase in the euphotic layer. Primary production and eventually grazing are stimulated. Biological aggregation inside fecal pellets conveys particles in the ocean interior where they are collected by sediment traps.

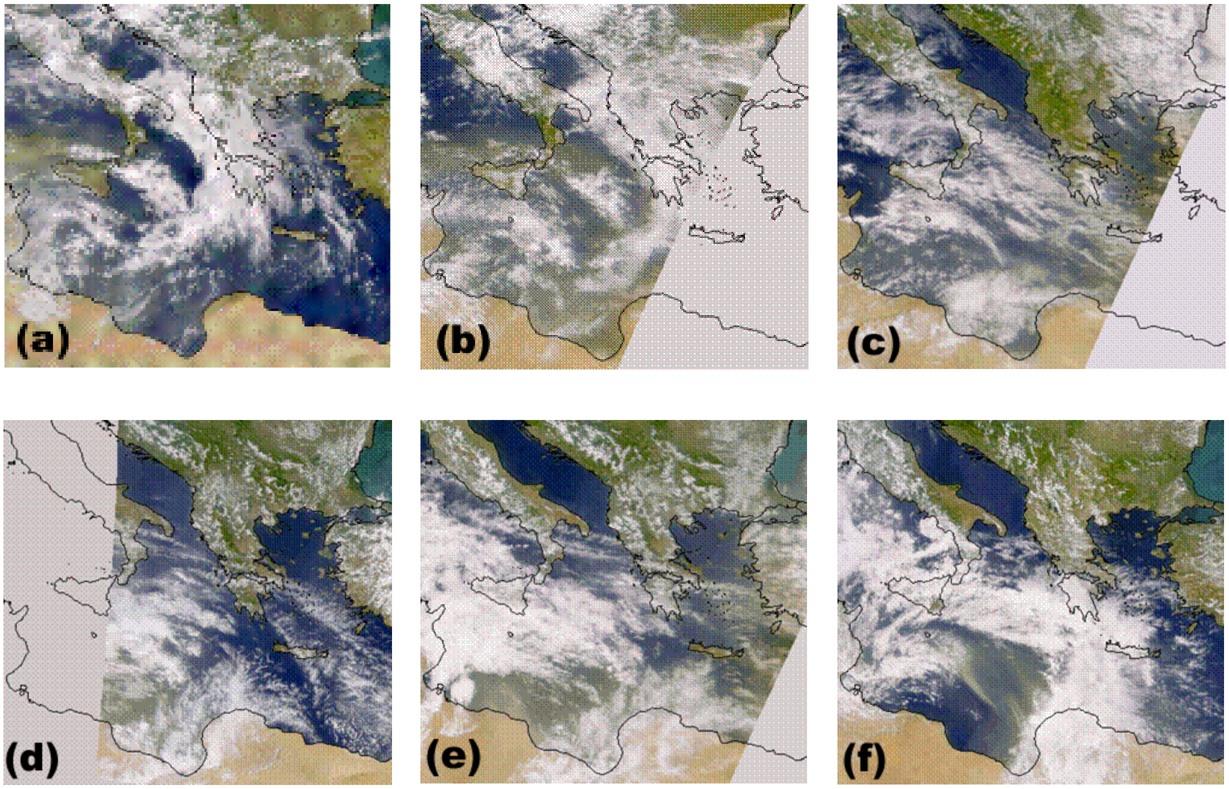

Figure 9 TrueColor Satellite images: (a) May 22nd, 2000 at 10:36 AM, (b) May 22nd, 2000 at 12:14 AM, (c) May 24th, 2000 at 12:02 AM, (d) May 26th, 2000 at 10:15 AM, (e) May 26th, 2000 at 11:51 AM, (f) May 27th, 2000 at 10:57 AM.

Sampling period	URANIA station		BANNOCK station
Mooring 1 September 15th, 1999 – June 2nd, 2000 Sampling resolution: 10-11 days	500 m depth	2800 m depth	2800 m depth
	TPF TCF	TPF TCF	TPF
Mooring 2 May 30th, 2000 – May 9th, 2001 Sampling resolution: 14-15 days	500 m depth		2800 m depth
	TPF TCF		TPF

Table 1 Urania and Bannock sediment trap general information. TPF=total particle flux [mg m^{-2} day^{-1}], TCF=total coccolith flux [nC m^{-2} day^{-1}].

<table>
<tr><td colspan="6">Correlation coefficients between current vertical velocity and particle fluxes</td></tr>
<tr><td colspan="2">URANIA Station</td><td>Degrees of freedom</td><td>No lag</td><td>1 lag</td><td>2 lags</td></tr>
<tr><td rowspan="4">Mooring 1</td><td>TPF at 500 m</td><td>21</td><td>0.4
*</td><td>0.63
***</td><td>n.s.</td></tr>
<tr><td>TCF at 500 m</td><td>21</td><td>0.75
***</td><td>0.63
***</td><td>0.51
**</td></tr>
<tr><td>TPF at 2800 m</td><td>21</td><td>0.55
***</td><td>0.51
**</td><td>0.56
***</td></tr>
<tr><td>TCF at 2800 m</td><td>12</td><td>0.7
***</td><td>0.61
**</td><td>0.67
***</td></tr>
<tr><td>Mooring 2</td><td>TPF at 500 m</td><td>19</td><td>0.45
**</td><td>0.42
*</td><td>0.39
*</td></tr>
<tr><td colspan="2">BANNOCK Station</td><td>Degrees of freedom</td><td>No lag</td><td>1 lag</td><td>2 lags</td></tr>
<tr><td>Mooring 1</td><td>TPF at 2800 m</td><td>9</td><td>0.53
*</td><td>n.s.</td><td>0.79
***</td></tr>
</table>

Table 2: Correlation coefficients between current vertical velocities and particle fluxes at the Urania and Bannock stations, with TPF=total particle flux [mg m^{-2} day^{-1}], TCF=total coccolith flux [nC m^{-2} day^{-1}]. The degrees of freedom - varying among the different time series - are shown in column 3. Correlation coefficients are computed on coincident time series (no lag) and on time series shifted of one (1 lag) and two (2 lags) sediment trap rotation intervals. Confidence intervals are depicted below the correlation coefficient values, with *=99%, **=95%, *=90%, and n.s.=not significant.**